atmosphere

Article

Assessing Spatiotemporal Characteristics and Driving Factors of Urban Public Buildings Carbon Emissions in China: An Approach Based on LMDI Analysis

Zhidong Zhang [1,*], Yisheng Liu [1] and Tian Ma [2]

1 School of Economics and Management, Beijing Jiaotong University, Beijing 100044, China; yshliu1@bjtu.edu.cn
2 School of Economics and Management, China University of Petroleum-Beijing, Beijing 102249, China; 20120637@bjtu.edu.cn
* Correspondence: zdzhang@bjtu.edu.cn

Abstract: Urban public buildings carbon emissions exhibit an upward trend and have a large potential in carbon emission reduction. The analysis of spatiotemporal characteristics and driving factors for urban public buildings carbon emissions is essential in formulating effective policies for carbon reduction, meeting commitments to peak carbon emissions and achieving carbon neutrality. This study takes China's urban public buildings carbon emissions as the research object, employing methods such as spatial autocorrelation analyses, kernel density estimation analyses, and the LMDI decomposition methods to explore the spatiotemporal characteristics and regional disparities in carbon emissions from 2006 to 2019. Furthermore, it quantifies the contributions of driving factors to the spatiotemporal changes in urban public buildings carbon emissions. The results show the following: (1) Urban public buildings carbon emissions among provinces are consistently increasing, indicating an overall upward trend. The spatial distribution highlights significant regional disparities. (2) The spatial characteristics of urban public buildings carbon emissions were basically stable. The eastern coastal regions demonstrate a high-high cluster, while the western regions exhibit a low-low cluster. The overall cluster evolution showed a decreasing trend from east to west. (3) Per capita urban public building area, economic density, urbanization rate, and population size serve as driving factors for carbon emissions from urban public buildings, while energy efficiency and energy consumption intensity act as inhibitory factors. The findings of this research can assist policymakers in getting a deeper comprehension of urban public buildings carbon emissions and providing a scientific basis to formulate appropriate carbon emission reduction policies.

Keywords: urban public buildings; carbon emissions; China; spatiotemporal characteristics; regional disparities; driving factors; LMDI decomposition

Citation: Zhang, Z.; Liu, Y.; Ma, T. Assessing Spatiotemporal Characteristics and Driving Factors of Urban Public Buildings Carbon Emissions in China: An Approach Based on LMDI Analysis. *Atmosphere* **2023**, *14*, 1280. https://doi.org/10.3390/atmos14081280

Academic Editors: Chong Wei, Chong Shi, Nan Li and Xingjun Xie

Received: 22 July 2023
Revised: 9 August 2023
Accepted: 11 August 2023
Published: 13 August 2023

1. Introduction

Carbon dioxide from global industrialization processes is the primary driving factor of global warming [1]. The United Nations Intergovernmental Panel on Climate Change has recommended limiting global warming to within 1.5 °C compared to pre-industrial levels to avoid catastrophic consequences [2]. Since 2009, China has held the position of the world's largest energy consumer and carbon emission emitter [3], which reached 9.89 billion tons in 2020, accounting for approximately 26.13% of global primary energy consumption. This is almost twice as much as the United States [4]. Being the world's greatest carbon emitter, China proactively undertakes the responsibility to reduce carbon emissions and has made a commitment to peak carbon emissions by 2030 and attain carbon neutrality by 2060 [5].

Buildings have emerged as one of the main contributors to China's carbon emissions [6], with particular attention paid to the role of public buildings. In 2020, the cumulative carbon emissions from the complete life cycle of buildings in China escalated to 5.08 billion tons, constituting a significant 50.9% portion of the nation's overall carbon emissions. The energy consumption of public buildings is generally higher than that of other types of buildings [7]. Urban public buildings generated 830 million tons of carbon emissions in the operational phase in 2020, which represented 38% of the overall carbon emissions in the operational phase of buildings [8]. Additionally, based on data from 2019 in China, the combined floor area of urban public buildings reached 13.6 billion square meters, resulting in 846 million tons of CO_2 emissions. The CO_2 emission intensity was recorded at 62.16 kg per square meter, which is nearly 2.5 times higher than that of urban residential buildings and 4 times higher than that of rural residential buildings [9]. The energy service demand in China's urban public buildings sector is projected to grow at a faster pace than in the residential sector. It is estimated to increase from 580 million tons of standard coal in 2020 to a range of 1.44–1.7 billion tons of standard coal by 2060, representing a growth rate of 1.5–1.7 times higher [10].

It is evident that urban public buildings have the greatest carbon emission potential compared to all other types of buildings [11]. However, this sector has received relatively little attention [12]. Considering that the carbon emission reduction potential in China's urban public buildings is greater than that in residential buildings, it is necessary for the government to formulate effective carbon emission control strategies for urban public buildings [13]. Additionally, substantial regional disparities in carbon emissions exist as a result of imbalances in regional economic development and variations in resource endowments [14]. If the reasons for significant disparities could be identified, it could help policymakers to develop differentiated mitigation policies for different regions [15]. Therefore, it is crucial to investigate the temporal patterns and spatial distribution changes of CO_2 emissions from a regional standpoint. In addition, there is a need to conduct further research on the driving factors that affect the energy consumption of urban public buildings. This will help to formulate reasonable carbon emission reduction responsibilities and specific carbon emission reduction measures.

To address the shortcomings of existing research, this paper aims to examine the spatiotemporal characteristics and regional disparities of urban public buildings carbon emissions, comprehensively decompose the driving factors, and establish a foundation for developing carbon emission reduction strategies adapted to different administrative areas. First, we conducted an investigation of the historical carbon emissions from provincial-level urban public buildings during the period of 2006–2019. The changes in urban public buildings carbon emissions in different regions were analyzed to explore the characteristics and evolutionary patterns. Second, the dynamic change of regional disparities was analyzed using kernel density estimation, and the global and local Moran's Index was calculated through spatial autocorrelation analysis to examine the spatial patterns. Finally, the Logarithmic Mean Divisia Index (LMDI) method was utilized to identify the key driving factors which influence urban public buildings carbon emissions. The contribution of each factor to the evolution of carbon emissions and regional disparities in urban public buildings was explored from a temporal and spatial perspective. Furthermore, this research summarizes carbon reduction measures and puts forward targeted policy recommendations to seek optimal decarbonization practices in the future, thereby providing insights for energy-saving and emission reduction in urban public buildings in China.

This study makes significant contributions in the following three primary aspects.

1. First, this study primarily investigates urban public buildings carbon emissions and constructs a research framework for the spatiotemporal distribution pattern of urban public buildings from 2006 to 2019. This is of great significance for expanding both the breadth and depth of study in the field of urban public buildings.
2. Second, through the use of kernel density estimation and spatial autocorrelation analysis, the spatial characteristics and dynamic evolution of regional urban public buildings carbon emissions are studied from a comprehensive perspective of temporal and spatial correlations, providing a more accurate understanding of the regional

characteristics of urban public buildings. This fills a previously identified research gap in the limited study of spatial characteristics of carbon emissions in the building sector.

3. Third, based on the spatiotemporal LMDI analysis method, the driving factors behind spatial disparities in urban public buildings carbon emissions are analyzed. We consider the impact of per capita urban public building area, population, urbanization rate, economic density, energy efficiency, and energy consumption intensity on urban public buildings carbon emissions in China. The driving mechanisms of these factors and regional disparities in urban public buildings carbon emissions are analyzed in depth. This research gives a theoretical foundation for policymakers to formulate CO_2 controlling policies for urban public buildings at the regional level. It is of great significance in balancing regional development and improving CO_2 reduction policies, contributing to the achievement of national goals regarding carbon peak and carbon neutrality.

The subsequent sections are organized as follows. Section 2 offers a comprehensive literature review. Section 3 provides the methodology and data source. Section 4 describes the results of spatiotemporal characteristic, regional disparities, and their driving factors for urban public buildings carbon emissions. Finally, Section 5 offers a conclusive summary of the study's findings and provides policy suggestions.

2. Literature Review

2.1. Spatiotemporal Analysis of Carbon Emission

In recent years, numerous scholars have conducted in-depth research on the spatiotemporal characteristics and regional disparities of carbon emissions. Han et al. [16] analyzed the regional disparities and decoupling evolution of carbon emissions by various provinces using the Tapio model. Li et al. [17] analyzed the regional emission differences in China through the LMDI model. Wang et al. [18] studied the evolutionary mechanisms and temporal and spatial heterogeneity of carbon emissions in the power sector. Liu et al. [19] investigated the spatiotemporal heterogeneity and regional disparities of CO_2 emissions within the transportation sector. Cui et al. [20] analyzed the regional differences and spatiotemporal dynamic evolution of planting industry in China over 20 years.

Moreover, many scholars have conducted studies on spatiotemporal characteristics of building sector in China. Liu et al. [21] examined the regional disparities in CO_2 emissions from buildings across different provinces. Wang et al. [22] studied the spatiotemporal patterns and changes, and driving factors associated with the pursuit of high-quality development in the building industry in China. Huo et al. [23] investigated the regional disparities in building carbon emissions from the perspectives of population, economy, and space. Li et al. [24] analyzed the spatiotemporal distribution and regional disparities of carbon emissions within the building sector, and found that the degree of inequality in public buildings is the highest. The existing research helps to reveal the regional disparities in China's carbon emissions and provides theory policy insights regarding limiting the growing trend of carbon emissions. However, there is relatively little research on the regional disparities in public buildings. In addition, addressing the issue of imbalanced regional development has emerged as a foundational principle for China's economic and social progress. Therefore, this study concentrates on the regional disparities in urban public buildings carbon emissions.

In the study of estimating regional disparities, scholars utilize the Theil index as a quantitative measure to assess regional disparities. Zhang et al. [25] used the Theil index to distinguish the impacts of different regions' CO_2 emissions on interregional and intraregional scales. Liu et al. [26] examined the characteristics of China's carbon emissions, regional disparities, causes, and the extent to which various factors influence carbon emissions, and found that industrial structure and urbanization are influencing factors causing emission disparities between regions. Gan et al. [27] delved into the discrepancy in carbon emission intensity within public buildings, examining the driving factors in two aspects: per capita carbon emissions and carbon emissions per unit of building area.

Although the Theil index is capable of indicating the level of regional inequality in carbon emissions, it treats the research objects as separate and homogeneous entities, overlooking their spatial relationships and interconnections [28]. Conversely, spatial autocorrelation analysis offers insights into spatial interdependence and autocorrelation among regions. Therefore, it is widely used in studies concerning spatial patterns and analyzing spatial heterogeneity [29]. Liu et al. [30] explored the spatiotemporal patterns of carbon emissions across different provinces in China using both global and local Moran's Index. Wang et al. [31] examined the CO_2 emissions of different provinces in China utilizing Moran's Index, revealing significant spatial correlation and distinctive spatial clustering characteristics. Li et al. [32] further applied spatial autocorrelation models to investigate the spatial autocorrelation of CO_2 emissions in 336 cities. They found that Shenzhen, Chengdu, and Guangzhou had a high level of coordination in CO_2 emissions. In addition, changes in regional differences can be observed qualitatively using kernel density estimation curves. Wang et al. [33] studied the spatiotemporal heterogeneity in building sector's emissions patterns through the kernel density estimation and Moran's Index. Li et al. [34] observed the changes in per capita CO_2 emissions and carbon intensity in building industry using kernel density estimation. Nonetheless, there remains a relatively limited advancement in terms of analyzing and visualizing regional disparities in carbon emissions within the building industry. Therefore, in order to reflect spatial disparities and correlation, this paper utilizes spatial autocorrelation analysis to assess the spatial variations in urban public buildings carbon emissions and uses kernel density estimation to examine the regional disparities and dynamic evolution of urban public buildings carbon emissions.

2.2. Driving Factors and Decomposition Method of Carbon Emissions

Within the building industry of China, some studies have endeavored to examine the factors that influence energy consumption and carbon emissions. Bai et al. [35] identified that factors such as investment scale, economic level, and population density serve as primary drivers for the growth of both national and provincial building energy consumption and emissions, while technology level and investment return rate were determined to be the main declining reasons. Li et al. [36] proposed that urbanization level, production efficiency, and energy efficiency are the inhibitory factors of carbon emissions in the building industry. According to Gong et al. [37], the primary driving factors behind energy consumption and carbon emissions are the growth in building areas, population, and urbanization. On the other hand, energy efficiency was identified as the main factor inhibiting carbon emissions. Jiang et al. [38] concludes six influencing factors of carbon emissions, including energy structure, energy intensity, economic level of the building industry, population density, and the proportion of new energy-saving area. Their findings indicated that the economic level plays a pivotal role in driving positive carbon emissions, while energy intensity serves as the primary factor influencing negative carbon emissions.

In research concentrated on the driving factors of carbon emissions, decomposition analysis—such as the IPAT framework, structural decomposition analysis (SDA), and index decomposition analysis (IDA)—is extensively employed.

The IPAT model, incorporating both the Kaya identity and the STIRPAT model, serves as the primary method for analyzing factors associated with carbon emissions. Kaya provides a more straightforward measurement method for carbon emissions within the framework of the IPAT model. It has gained extensive usage in decomposing carbon emissions, assessing carbon intensity, and analyzing other relevant factors [27]. Shahbaz et al. [39] employed the STIRPAT model to examine the impacts of various factors on carbon emissions. The research findings highlight that urbanization and economic growth constitute the primary drivers of carbon emissions. Nasir et al. [40] conducted an analysis of the effects of various socioeconomic factors on carbon emissions through the STIRPAT model, including economic growth, trade openness, industrialization, and energy consumption.

SDA encompasses both additive and multiplicative forms, providing a framework for studying the influence factors of carbon emission on the production side [41,42]. Rose et al. [43] examined the theoretical foundation and main characteristics of SDA. Hong et al. [44] employed the SDA method to assess the impacts of driving factors on energy growth in building industry between 1990 and 2012. The findings revealed that increased demand and reduced energy intensity had a notable influence on carbon emissions. Liu et al. [45] employed SDA and revealed that the optimization of the industrial structure had a pronounced restraining impact on CO_2 emissions in building industry, with final demand playing an absolutely dominant role in increasing CO_2 emissions. Shi et al. [46] employed the SDA to delve into influencing factors and their contributions to the dynamic changes in carbon emissions in construction industry. The results unveiled that the final demand and energy intensity had the most significant impact on carbon emissions changes. Xu et al. [47] examined the driving factors behind consumption-based emissions in Guangdong province using SDA. They found that the consumption structure, consumption per capita, and population effect played a promoting role in embodied emissions. Conversely, the emission intensity effect emerged as the most significant mitigating factor across all sectors.

Compared to SDA, IDA stands out with its advantage of requiring less data and offering greater flexible analysis periods [48]. Among them, one of the most commonly used IDA methods is the LMDI. This model has a simple calculation process, decomposes residuals that are interpretable, and enables comprehensive decomposition, making it widely applied in empirical research [49–51]. Ang et al. [52] assessed different IDA methods, and ultimately determined that LMDI is favored because of the solid theoretical basis, simplicity of use, and interpretability of results. After the initial application of the LMDI method to analyze industrial carbon emissions by Ang et al. [53], an increasing number of scholars started to conduct decomposition analyses of energy-related carbon emissions. Jiang et al. [54] utilized the LMDI method to examine the driving factors behind changes in carbon emissions within China's building industry. Ma et al. [55] reported an LMDI model based on the IPAT framework to investigate the driving factors that influence building energy efficiency. Lin et al. [56] used LMDI to explore the potential for carbon emission reduction in China's building industry. The findings indicated that energy intensity is the major driving factor for carbon emissions reduction.

The above literature mainly focuses on the carbon reduction potential and driving factors of China's building industry, but there exists a notable absence of comprehensive investigation into the specific driving factors related to China's urban public buildings. Considering the limitations and incompleteness of statistical data in China and recognizing the applicability and advantages of the LMDI method in exploring driving factors of carbon emissions in building industry, this study utilizes LMDI as a decomposition tool to explore urban public buildings carbon emissions.

3. Methodology and Data Source

3.1. Kernel Density Estimation

Kernel density estimation is a non-parametric estimation method used to measure the probability density function of a random variable based on a set of observed data points. By employing a smooth peak function, kernel density estimation provides insights into the distribution shape of the data [57]. When associated with the temporal changes in data, it becomes possible to characterize and visualize the spatiotemporal distribution shape of urban public buildings carbon emissions, revealing the dynamic evolution over time. The kernel density formula is as follows:

$$f_h(x) = \frac{1}{nh}\sum_{i=1}^{n} K(\frac{x - x_i}{h}) \quad (1)$$

$K(\frac{x-x_i}{h})$ is Gaussian kernel function. The expression can be represented as follows.

$$K(x) = \frac{1}{\sqrt{2\pi}} \exp(-\frac{1}{2}x^2) \quad (2)$$

where n represents the number of regions, h represents the bandwidth. The value of the bandwidth determines the smoothness of the kernel density estimation function. A smaller bandwidth leads to less smoothing, while a larger bandwidth leads to a flatter curve [58].

3.2. Spatial Autocorrelation Analysis

Spatial autocorrelation analysis is a method utilized to quantify the similarity of attribute values between a specific region and its neighboring regions [34]. It can systematically measure the aggregation and dispersion and reveal the spatiotemporal characteristics of urban public buildings carbon emissions in China. Spatial autocorrelation analysis can be categorized into two types based on the research scope: global spatial autocorrelation and local spatial autocorrelation.

Global spatial autocorrelation reflects the overall level of spatial correlation within a regional space [59]. This study utilizes the global Moran's Index to assess the overall spatial autocorrelation of China's urban public buildings carbon emissions. The calculation [35] formula is shown in Equation (3).

$$I_{global} = \frac{\sum_{i=1}^{n}\sum_{j=1}^{n} w_{ij}(x_i - \overline{x})(x_j - \overline{x})}{S^2 \sum_{i=1}^{n}\sum_{j=1}^{n} w_{ij}} \quad (3)$$

$$S^2 = \frac{1}{n}\sum_{i=1}^{n}(x_i - \overline{x})^2 \quad (4)$$

where n denotes the number of regions. x_i and x_j denote the carbon emission values of regions i and j. $\overline{x} = \frac{1}{n}\sum_{i=1}^{n} x_i$ represents the average value of carbon emission across all regions. w_{ij} represents the element of the spatial weight matrix. Specifically, the global Moran's Index $\in [-1, 1]$.

For this research, the spatial weight matrix is defined using queen contiguity. If two regions share an edge or node, their corresponding dummy variable is set to 1; otherwise, it is set to 0. Moran's Index value close to 1 suggests a higher level of spatial aggregation, while the value close to -1 indicates a random distribution of carbon emissions and the absence of spatial correlation [60].

Compared to the global Moran's Index, local spatial autocorrelation is utilized when there is a need to reflect the extent of correlation between individual spatial units and their neighbors for a specific attribute from a more detailed micro-level perspective [61]. The calculation of local Moran's Index is shown in Equation (5).

$$I_{local} = \frac{(x_i - \overline{x})^2}{S^2}\sum_{j=1}^{n} w_{ij}(x_j - \overline{x}) \quad (5)$$

There are four types in local Moran's index results, including high and high (H-H), low and high (L-H), low and low (L-L), and high and low (H-L). Significant similarity is indicated by H-H or L-L, implying that areas with high values are surrounded by areas with high values or areas with low values are surrounded by areas with low values. Conversely, significant dispersion is indicated by L-H or H-L, representing that areas with high values are surrounded by areas with low values or areas with low values are surrounded by areas with high values, respectively [62]. When in a Moran scatterplot, the first quadrants (H-H) and third quadrants (L-L) represent positive spatial correlations between samples, while the second (L-H) quadrants and fourth quadrants (H-L) represent negative spatial correlations.

3.3. LMDI Decomposition Model

Index Decomposition Analysis is widely used in studies on CO_2 emission changes, especially suitable for decomposition models with fewer variables or limited time series data. In this study, we combine the factor selection approach based on the Kaya model with the LMDI method to analyze the key driving factors of urban public buildings carbon emissions in China. Combined with the characteristics of urban public buildings, carbon emissions are decomposed into the following influencing factors, as depicted in Equation (6).

$$C = \frac{C}{E} \times \frac{E}{GDP} \times \frac{GDP}{A} \times \frac{A}{P_{urban}} \times \frac{P_{urban}}{P} \times P = \Delta C_{ee} \times \Delta C_{eci} \times \Delta C_{eco} \times \Delta C_{area} \times \Delta C_{ur} \times \Delta C_{pop} \quad (6)$$

where C represents urban public buildings carbon emissions, E represents the corresponding energy consumption, GDP refers to Gross Domestic Product, A denotes the total urban public buildings area, P_{urban} denotes the urban population, and P represents the total population.

Up to now, the LMDI method has been widely utilized in the analysis of carbon emission driving factors through index decomposition. It decomposes an aggregative indicator into several relevant driving factors and quantifies their respective contributions to the changes in the aggregate indicator. We employed the LMDI method to quantify six factors' contributions to the temporal and spatial variations in urban public buildings carbon emissions, as shown in Equation (7).

$$\Delta C = C^T - C^0 = \Delta C_{ee} + \Delta C_{eci} + \Delta C_{eco} + \Delta C_{area} + \Delta C_{ur} + \Delta C_{pop} \quad (7)$$

where C^T and C^0 denote the carbon emissions from China's urban public buildings in the T-th year and the base year (phase 0). ΔC_{ee}, ΔC_{eci}, ΔC_{eco}, ΔC_{area}, ΔC_{ur}, ΔC_{pop} represent the impacts of the six factors on the temporal changes in carbon emissions from China's urban public buildings. The calculation [63] can be performed according to Equations (8)–(13).

$$\Delta C_{ee} = \frac{C^T - C^0}{\ln C^T - \ln C^0} \ln(\frac{{C_{ee}}^T}{{C_{ee}}^0}) \quad (8)$$

$$\Delta C_{eci} = \frac{C^T - C^0}{\ln C^T - \ln C^0} \ln(\frac{{C_{eci}}^T}{{C_{eci}}^0}) \quad (9)$$

$$\Delta C_{eco} = \frac{C^T - C^0}{\ln C^T - \ln C^0} \ln(\frac{{C_{eco}}^T}{{C_{eco}}^0}) \quad (10)$$

$$\Delta C_{area} = \frac{C^T - C^0}{\ln C^T - \ln C^0} \ln(\frac{{C_{area}}^T}{{C_{area}}^0}) \quad (11)$$

$$\Delta C_{ur} = \frac{C^T - C^0}{\ln C^T - \ln C^0} \ln(\frac{{C_{ur}}^T}{{C_{ur}}^0}) \quad (12)$$

$$\Delta C_{pop} = \frac{C^T - C^0}{\ln C^T - \ln C^0} \ln(\frac{{C_{pop}}^T}{{C_{pop}}^0}) \quad (13)$$

3.4. Data Source

In order to conduct in-depth research and discussion on urban public buildings carbon emissions, this study calculates the total urban public buildings carbon emissions in China and analyzes the changes in regional variations of carbon emissions through kernel density estimation. Then, dynamic evolution characteristics of the spatial patterns is explored by combining with spatial autocorrelation analysis, and the contributions of driving factors to spatiotemporal changes and differences are measured by LMDI analysis. Finally, we examine the impact of factors such as energy efficiency, energy consumption intensity, economic density, per capita public building area, urbanization rate, and population on urban public buildings carbon emissions.

China has a total of 34 administrative regions. However, due to data limitations, the statistical analysis includes 30 administrative regions, excluding Tibet, Taiwan, Hong Kong, and Macau. Additionally, this study classifies the 30 administrative regions into four distinct regions: Eastern, Central, Western, and Northeastern regions, based on data from the National Bureau of Statistics. It is illustrated in Table 1.

Table 1. Division of four major regions in China.

Region	Province Included in the Region
East region	Beijing, Tianjin, Hebei, Shanghai, Jiangsu, Zhejiang, Fujian, Shandong, Guangdong, Hainan
Central region	Shanxi, Anhui, Jiangxi, Henan, Hubei, Hunan
West region	Inner Mongolia, Guangxi, Chongqing, Sichuan, Guizhou, Yunnan, Shaanxi, Gansu, Qinghai, Ningxia, Xinjiang
Northeast region	Liaoning, Jilin, Heilongjiang

This study uses the calculation method for building energy consumption [64]. Considering the limitations of data availability and completeness, the calculation of urban public buildings carbon emissions covers the period from 2006 to 2019. The data for total population, urban population, and GDP were acquired from the China Statistical Yearbook. The data for public buildings area were obtained from China Building Energy and Emissions Database (CBEED). The data associated with energy consumption were obtained from the regional energy balance sheets within China Energy Statistical Yearbook.

4. Results and Discussion

4.1. Urban Public Buildings Carbon Emissions

Table 2 presents the carbon emissions of urban public buildings in 30 provinces in China from 2006 to 2019. Overall, during this period, there was an increasing trend in urban public buildings carbon emissions among all provinces. Provinces that experienced a significant increase include Hebei, Shanxi, Inner Mongolia, Liaoning, Heilongjiang, Jiangsu, Zhejiang, Anhui, Fujian, Jiangxi, Shandong, Henan, Hubei, Hunan, Guangdong, Sichuan, Guizhou, Yunnan, and Shaanxi. On the other hand, provinces that experienced relatively modest increase include Beijing, Tianjin, Jilin, Shanghai, Guangxi, Hainan, Chongqing, Gansu, Qinghai, Ningxia, and Xinjiang.

Figure 1 shows the gross amount and growth rate of urban public buildings carbon emissions from 2006 to 2019. The carbon emissions rose from 401 million tons in 2006 to 853.23 million tons in 2019. The total carbon emissions more than doubled during this period. However, the gross urban public buildings carbon emissions exhibited a declining trend, with the growth rate gradually decreasing from 7.4% to 1.2%. In 2014, there was a significant decrease in gross carbon emissions, dropping from 771.52 million tons to 748.65 million tons.

Figure 2 illustrates the temporal changes trend of per capita urban public buildings carbon emissions. From 2006 to 2019, the per capita urban public buildings carbon emissions rose from 310.27 kg per capita to 607.52 kg per capita, demonstrating an average annual growth rate of 5.3%. Further analysis revealed that the per capita urban public buildings carbon emissions exhibited a stable upward trend. In 2010 and 2013, there were rapid increases in per capita urban public buildings carbon emissions, while a slight decline was observed in 2014, and variations in other periods were not significant. Overall, there was a consistent and substantial growth in both the total and per capita urban public buildings carbon emissions.

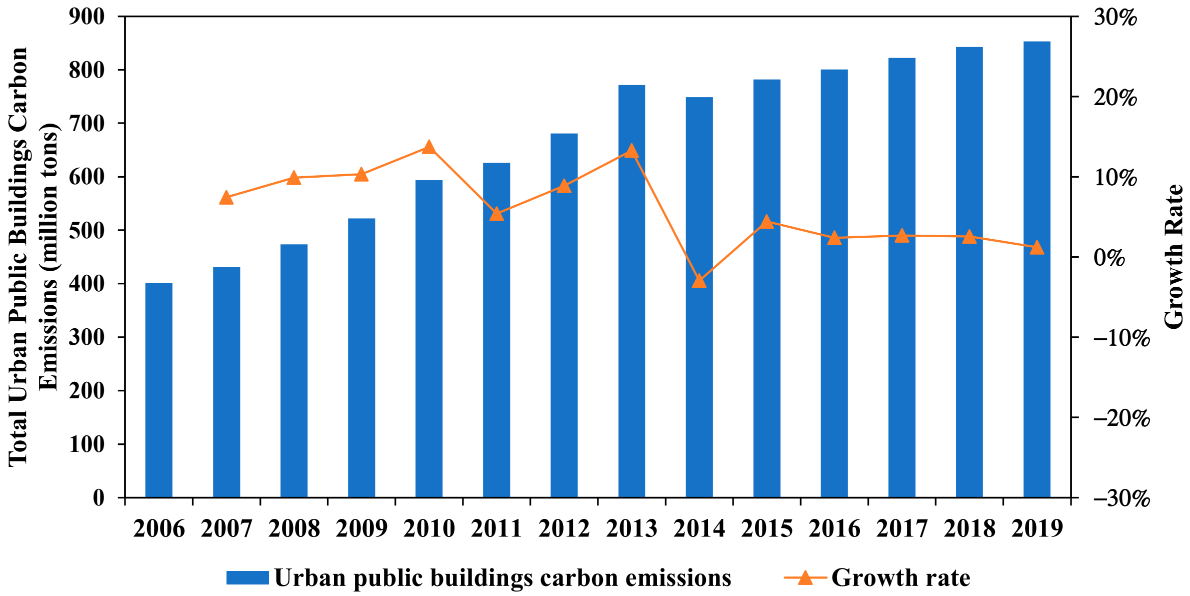

Figure 1. Total urban public buildings carbon emissions.

Table 2. Urban public buildings carbon emissions in China's 30 provinces from 2006–2019 (million tons).

	2006	2007	2008	2009	2010	2011	2012	2013	2014	2015	2016	2017	2018	2019
Beijing	35.35	35.89	43.52	47.17	44.82	48.41	53.17	51.13	50.10	49.82	51.17	44.84	44.72	43.83
Tianjin	11.71	12.28	12.85	13.22	15.02	15.71	16.90	16.44	16.06	16.24	17.39	17.48	17.40	17.81
Hebei	20.91	21.85	22.39	32.39	36.33	38.63	40.37	40.53	40.59	43.23	44.82	42.33	42.37	44.71
Shanxi	15.01	21.50	17.54	31.81	26.63	26.79	27.80	26.68	26.84	27.68	26.34	27.94	27.51	26.61
Inner Mongolia	18.70	21.08	22.20	36.69	45.39	48.01	59.04	63.45	67.47	65.26	51.61	33.59	41.30	41.46
Liaoning	24.19	25.42	26.37	39.14	31.25	34.93	38.32	37.73	38.14	41.75	42.22	41.62	41.56	38.20
Jilin	20.97	20.92	21.43	19.95	24.05	23.08	24.55	30.99	29.37	35.01	35.80	30.89	22.22	21.56
Heilongjiang	19.10	19.60	29.67	19.41	19.92	32.89	38.43	49.02	52.32	66.83	71.22	66.64	53.87	48.43
Shanghai	23.12	27.87	29.43	30.52	1.32	33.49	34.74	35.13	32.12	30.90	31.33	32.12	32.65	33.35
Jiangsu	25.49	24.72	29.15	26.98	32.67	37.14	41.75	37.62	34.93	35.68	38.11	42.11	47.20	48.22
Zhejiang	27.51	26.61	28.88	38.47	42.11	30.26	34.15	43.01	43.55	38.28	35.31	37.06	39.23	41.02
Anhui	6.45	7.61	9.14	10.15	11.28	13.23	14.91	17.15	16.30	17.54	18.16	19.98	20.27	23.07
Fujian	9.89	10.39	11.15	11.27	11.72	13.58	14.16	14.41	14.50	14.59	15.64	17.06	18.74	19.37
Jiangxi	5.34	3.89	4.48	8.23	10.36	13.18	9.93	10.66	11.57	9.96	11.14	13.02	14.94	15.49
Shandong	35.47	37.72	37.27	54.87	61.65	66.07	76.45	58.01	54.71	55.81	56.70	56.24	50.37	52.23
Henan	11.06	11.14	11.51	12.83	13.68	20.41	22.59	24.09	22.90	25.86	29.65	23.76	30.99	32.91
Hubei	12.19	13.75	15.80	24.95	30.32	41.02	39.49	28.95	28.39	29.48	30.03	31.52	33.82	35.28
Hunan	12.03	16.27	17.63	21.91	23.95	25.47	28.20	23.53	31.93	34.34	37.56	40.96	35.85	37.17
Guangdong	42.20	44.67	45.78	52.60	48.47	58.83	62.90	67.61	64.42	65.35	68.05	72.09	78.18	77.81
Guangxi	10.10	6.50	7.20	8.48	8.71	9.77	10.66	9.21	9.45	10.17	10.23	11.07	12.17	13.15
Hainan	2.13	2.25	2.61	3.03	3.13	3.59	4.18	5.69	4.39	4.66	5.02	5.53	6.41	7.06
Chongqing	5.05	5.19	5.57	7.71	8.87	9.31	11.44	10.05	11.06	7.95	12.64	10.95	13.88	14.86
Sichuan	8.45	10.74	21.05	13.57	14.57	19.70	20.40	26.40	24.69	25.62	26.83	94.77	32.69	30.97
Guizhou	10.39	10.76	11.01	25.35	25.94	26.95	27.93	43.36	45.32	49.05	48.48	50.83	44.42	41.22
Yunnan	4.13	3.99	3.99	6.42	7.44	9.72	11.72	12.02	14.34	14.79	15.83	16.23	18.41	18.82
Shaanxi	12.79	12.00	12.53	16.28	18.06	19.57	20.85	18.98	19.40	19.28	19.44	19.49	20.37	21.42
Gansu	7.74	7.97	13.35	10.94	10.85	8.55	9.52	10.85	10.50	10.92	12.75	12.19	13.13	13.89
Qinghai	2.85	2.78	2.29	3.69	4.06	4.12	4.35	4.25	3.61	4.16	4.48	6.25	6.87	6.90
Ningxia	3.09	3.40	2.81	4.35	4.59	4.16	4.78	3.88	4.18	4.18	5.06	4.58	4.64	5.69
Xinjiang	14.41	16.46	16.38	14.34	15.67	16.39	17.42	17.15	17.61	19.40	21.77	22.37	22.76	23.15

Figure 3 displays the temporal changes trend of urban public buildings carbon emissions in four main regions of China. The carbon emissions in the eastern coastal region were notably higher compared to other regions. From 2006 to 2019, the eastern coastal region witnessed an increase in urban public buildings carbon emissions from 233.8 million tons to 385.4 million tons, demonstrating an average annual growth rate of 3.92%. The carbon emissions in the northeastern region increased from 64.26 million tons in 2006 to 108.2 million tons in 2019. Urban public buildings carbon emissions in the central regions and western regions have grown rapidly, with an average annual increase rate of 8.09% and 6.86%, respectively.

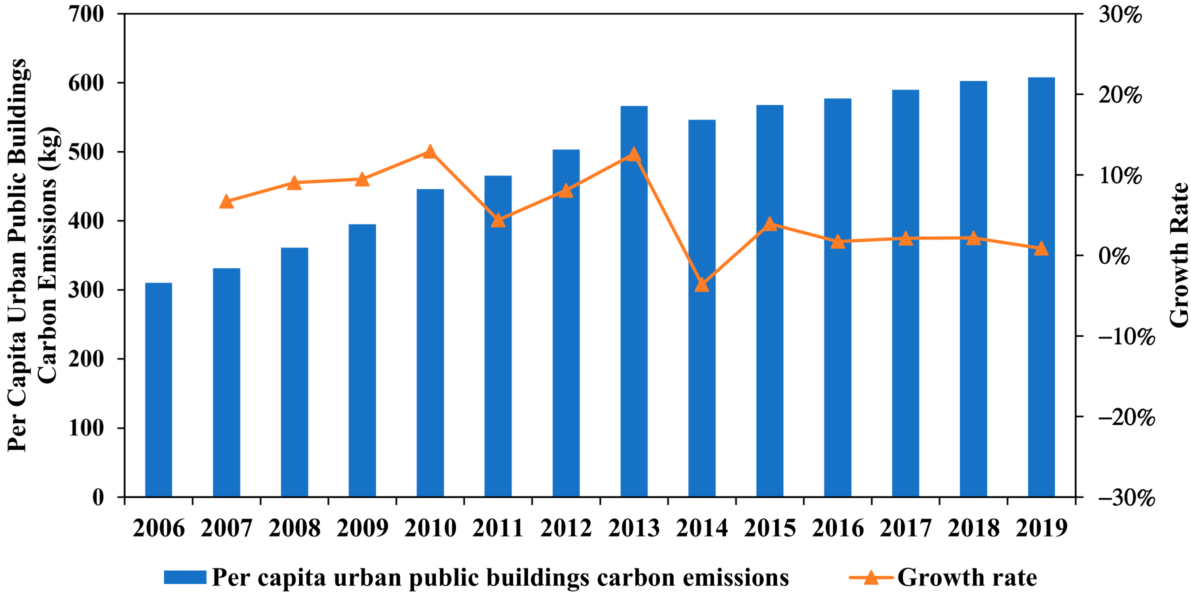

Figure 2. Per capita urban public buildings carbon emissions.

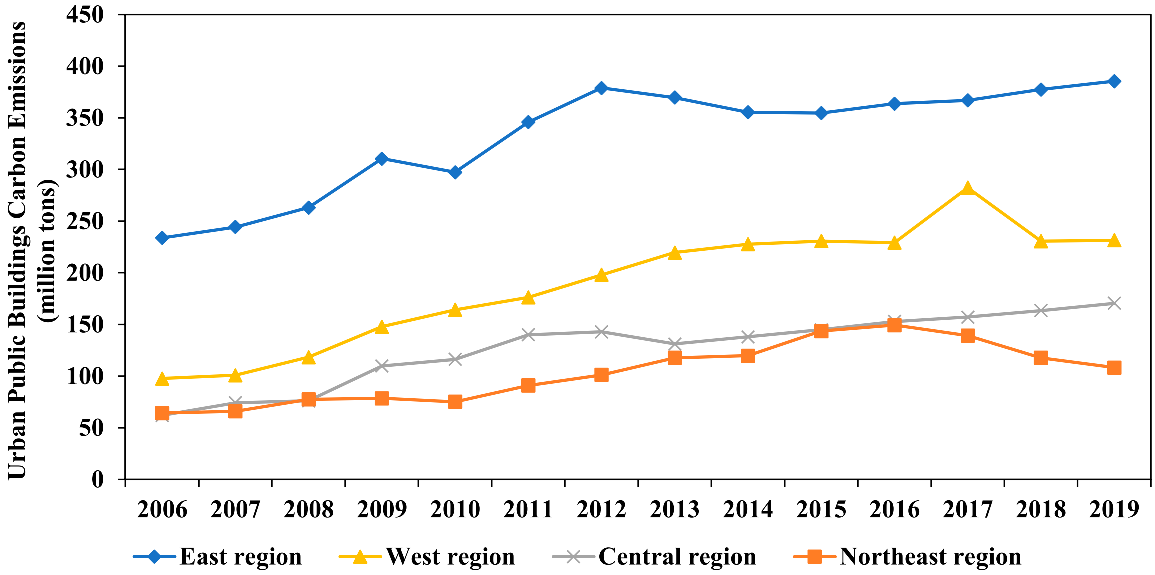

Figure 3. Temporal changes of urban public buildings carbon emission in four major regions.

Figure 4 illustrates the temporal change trend of per capita urban public buildings carbon emissions from in four main regions of China. There is a certain level of disparity among these regions. The northeastern region is at the forefront, with per capita emissions increasing from 594.1 kg in 2006 to 1084.1 kg in 2019. The eastern coastal region and western region are in the second tier. The central region has relatively lower per capita urban public buildings carbon emissions.

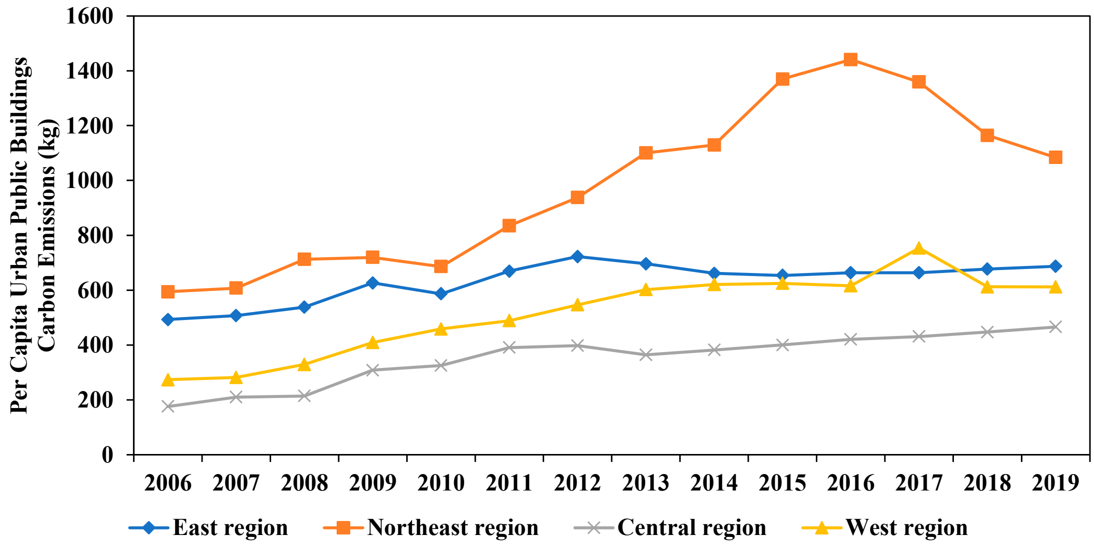

Figure 4. Temporal changes of per capita urban public buildings carbon emission in four major regions.

Figure 5 shows 30 provinces' urban public buildings carbon emissions in 2006 and 2019. It can be seen that during the period of 2006–2019, the majority of regions experienced a significant increase in urban public buildings carbon emissions and exhibit different trajectories. Among the regions, Guangdong, Guizhou, Heilongjiang, Hunan, Hebei, Hubei, and Inner Mongolia had the largest growth in total urban public buildings carbon emissions. Specifically, Guangdong witnessed a significant increase, rising from 42.2 million tons in 2006 to 77.8 million tons in 2019, representing a growth of 35.6 million tons. Additionally, Yunnan, Guizhou, Sichuan, Chongqing, Anhui, Hunan, Henan, Jiangxi, and Hubei experienced significant increases in carbon emissions from urban public buildings. Among them, Yunnan and Guizhou provinces had the highest growth rates in total urban public buildings carbon emissions, with average annual growth rates of 12.37% and 11.18%, respectively.

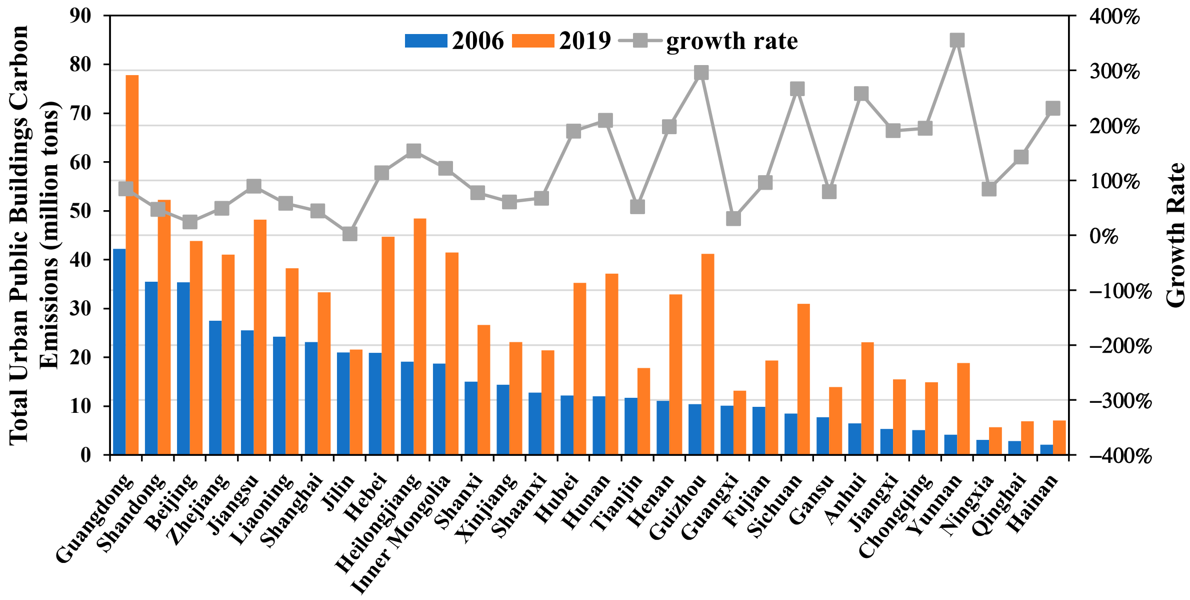

Figure 5. Urban public buildings carbon emissions in China's 30 provinces.

In contrast, there were only slight increases in the total urban public buildings carbon emissions in Beijing, Guangxi, Shanghai, Shandong, Zhejiang, and Tianjin. The overall spatial distribution pattern exhibits higher levels in the eastern and northern regions, while lower levels are observed in the western and southern regions.

4.2. Kernel Density Estimation Analysis

Figure 6 depicts the spatiotemporal characteristics of urban public buildings carbon emissions. As a non-parametric method, kernel density estimation portrays the distribution pattern characteristics of a random variable by means of a continuous density curve. The horizontal axis represents carbon emissions values, while the vertical axis represents density.

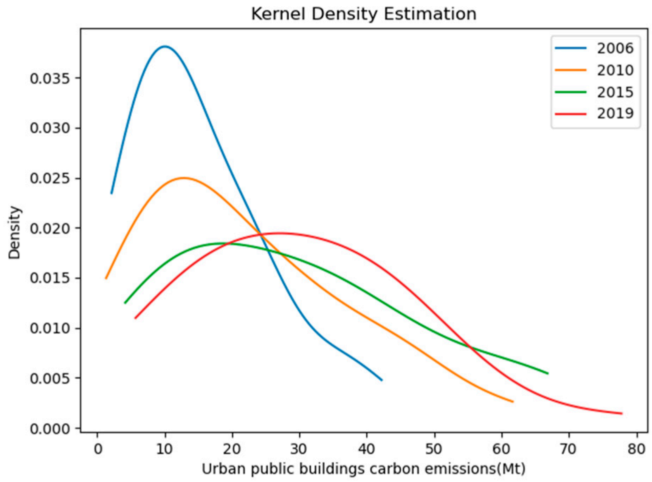

Figure 6. Dynamic spatiotemporal characteristics evolution process of urban public buildings carbon emissions in 2006–2019.

The distribution of urban public buildings carbon emissions changes over time. Overall, the kernel density estimation curve exhibits a single-peaked distribution, with its center continuously shifting to the right and the peak gradually declining. The distribution curve's left tail continues to shift marginally toward the right, while the right tail changes dramatically toward the right, and the interval continues to widen. The results indicate that in 2010, 2015, and 2019, high-value areas of urban public buildings carbon emissions experienced gradual growth compared to 2006, and these high-value areas consistently expanded. Specifically, when comparing 2010 to 2006, the wave shape transformed from an abrupt summit to a wider summit, with the summit exhibited a clear downward and rightward trend. The fluctuations in the tail of curve between 2010 and 2015 decreased, indicating a decrease in the clustering of areas with higher emission values. In 2010, 2015, and 2019, the distribution curves of urban public buildings carbon emissions have a similar trend, a diminishing summit, a shifting curve towards the right, and a widened range of variation.

As the distribution curve transformed from being tall and thin to short and broad, it indicated an expanding trend in regional disparities in urban public buildings carbon emissions. The main reasons for this change in trend are as follows. Imbalanced economic development has led to widening regional disparities in carbon emissions from urban public buildings between eastern and western China. The economic expansion in eastern China is faster than in the western regions, which is related to the increase in urban income, energy demand, and carbon emissions. Due to the relatively developed economy in the east, the income of urban residents has increased, resulting in a rise in energy demand and subsequent growth in carbon emissions. Climate difference is also another factor that influences urban public buildings carbon emissions. The northern regions have extremely cold winters and primarily rely on large-scale centralized heating systems, which often use coal and result in higher carbon emissions. In contrast, in the southern regions, air conditioning or electric heaters are commonly used throughout the winter, leading to regional differences in energy consumption compared to the northern regions.

4.3. Spatial Autocorrelation Analysis

4.3.1. Global Spatial Autocorrelation Analysis

Figure 7 shows the results of global spatial autocorrelation analysis for urban public buildings carbon emissions. With the exception of 2017, Moran's Index for urban public buildings carbon emissions is consistently greater than zero, suggesting a moderate positive spatial correlation between the regions. Over time, the Moran's Index of urban public buildings carbon emissions exhibit a decreasing trend, followed by stabilization. It decreased from 0.369 in 2006 to 0.077 in 2010. Subsequently, the Moran's Index fluctuates around 0.1. It can be seen that the regional disparities in urban public buildings carbon emissions show an expanding trend, which is consistent with the results obtained from kernel density estimation analysis. The Moran's Index was found to be significant at 5% level from 2006 to 2013. However, from 2014 to 2019, it did not pass the 5% significance level test, indicating that carbon emissions in those years exhibited a random distribution. This reveals that the regional disparities in urban public buildings carbon emissions exhibited a trend of initially expansion and followed by stabilization during the study period.

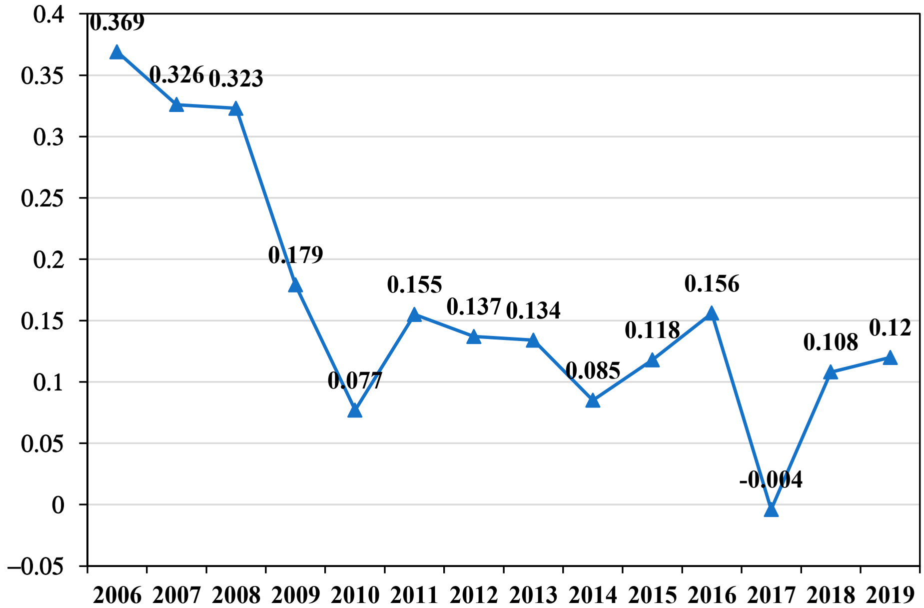

Figure 7. Global Moran's Index for urban public buildings carbon emissions in 30 provinces.

4.3.2. Local Spatial Autocorrelation Analysis

Global Moran's Index merely reveals the overall characteristics of urban public buildings carbon emissions in China. However, it fails to explain the individual characteristics of each region. Therefore, this study combines Moran scatter plots and local indicators of spatial association to further investigate the local spatiotemporal evolution characteristics of urban public buildings carbon emissions.

Figure 8 provides an overview of China's 30 provinces Moran scatterplots for urban public buildings carbon emissions in 2006, 2011, 2015, and 2019. It can be seen that most provinces are located in quadrants I (H-H clusters) and quadrants III (L-L clusters), representing more than 70% of all provinces. Less than 30% of provinces are located in quadrants II (L-H type) and quadrants IV (H-L type). The result shows that provinces with high urban public buildings carbon emissions are adjacent to other provinces with high carbon emissions, whereas those with low urban public buildings carbon emissions are adjacent to other provinces with low carbon emissions. By examining the slopes of the lines in different years, it becomes evident that local areas exhibit positive spatial autocorrelation in urban public buildings carbon emissions. Overall, the provincial spatial clustering pattern of urban public buildings carbon emissions mainly shows a positive correlation.

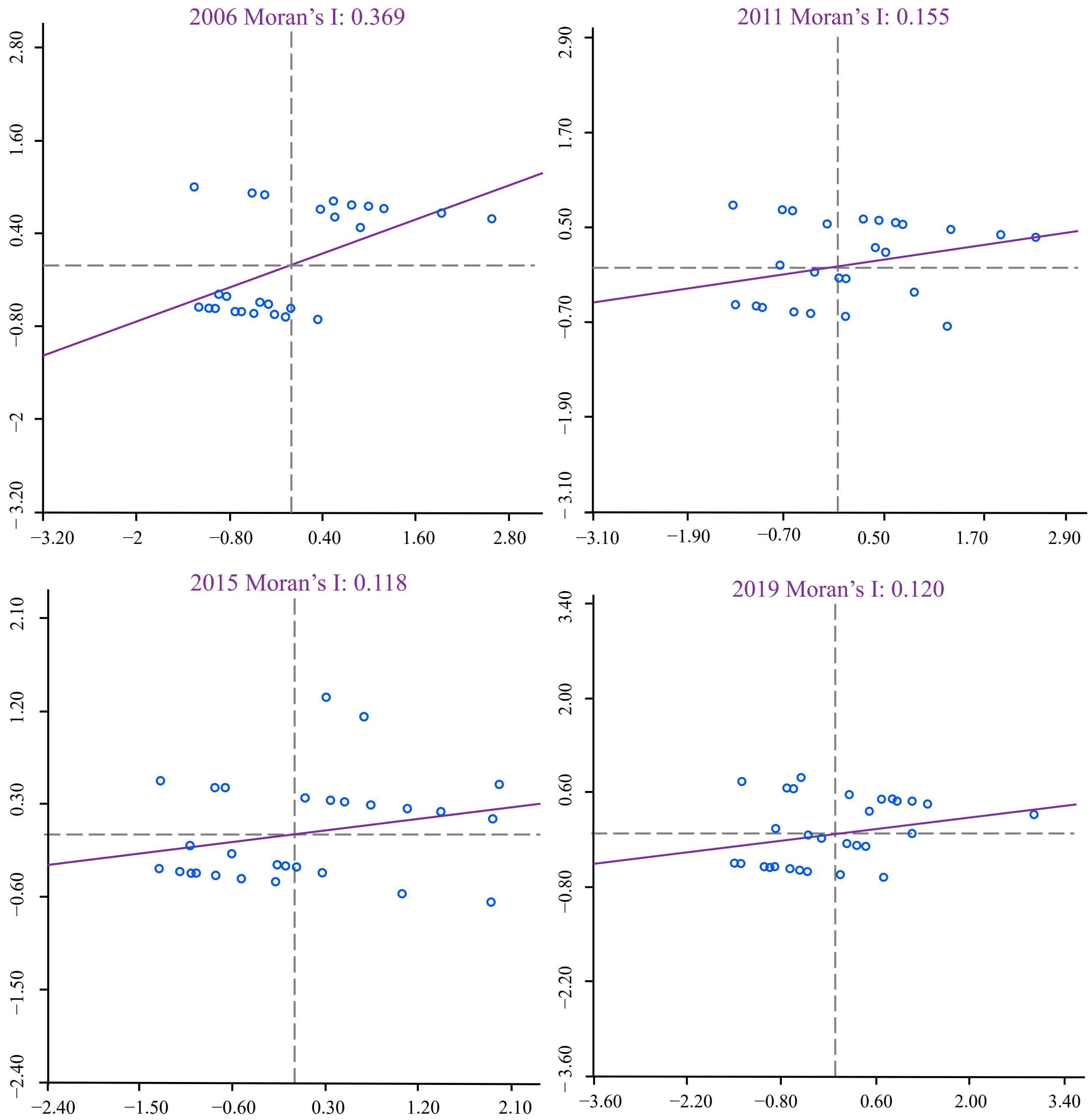

Figure 8. Moran scatterplots of urban public buildings carbon emissions among 30 provinces in 2006, 2011, 2015, 2019.

The local indicators of spatial association are utilized to depict the local spatial distributions. In order to better identify the spatial clustering changes among the 30 provinces, Figure 9 plotted aggregated distribution maps of urban public buildings carbon emissions in 2006, 2010, 2015, and 2019.

In 2006, the provinces classified as H-H and L-L clusters for carbon emissions accounted for 80.95% of the significantly classified provinces. In 2010 and 2015, they accounted for 60% and 33.34% of the significantly classified provinces, respectively. In 2019, they accounted for 71.42% of the significantly classified provinces. This result fully indicates that the major H-H cluster provinces dominate the spatial pattern of urban public buildings carbon emissions.

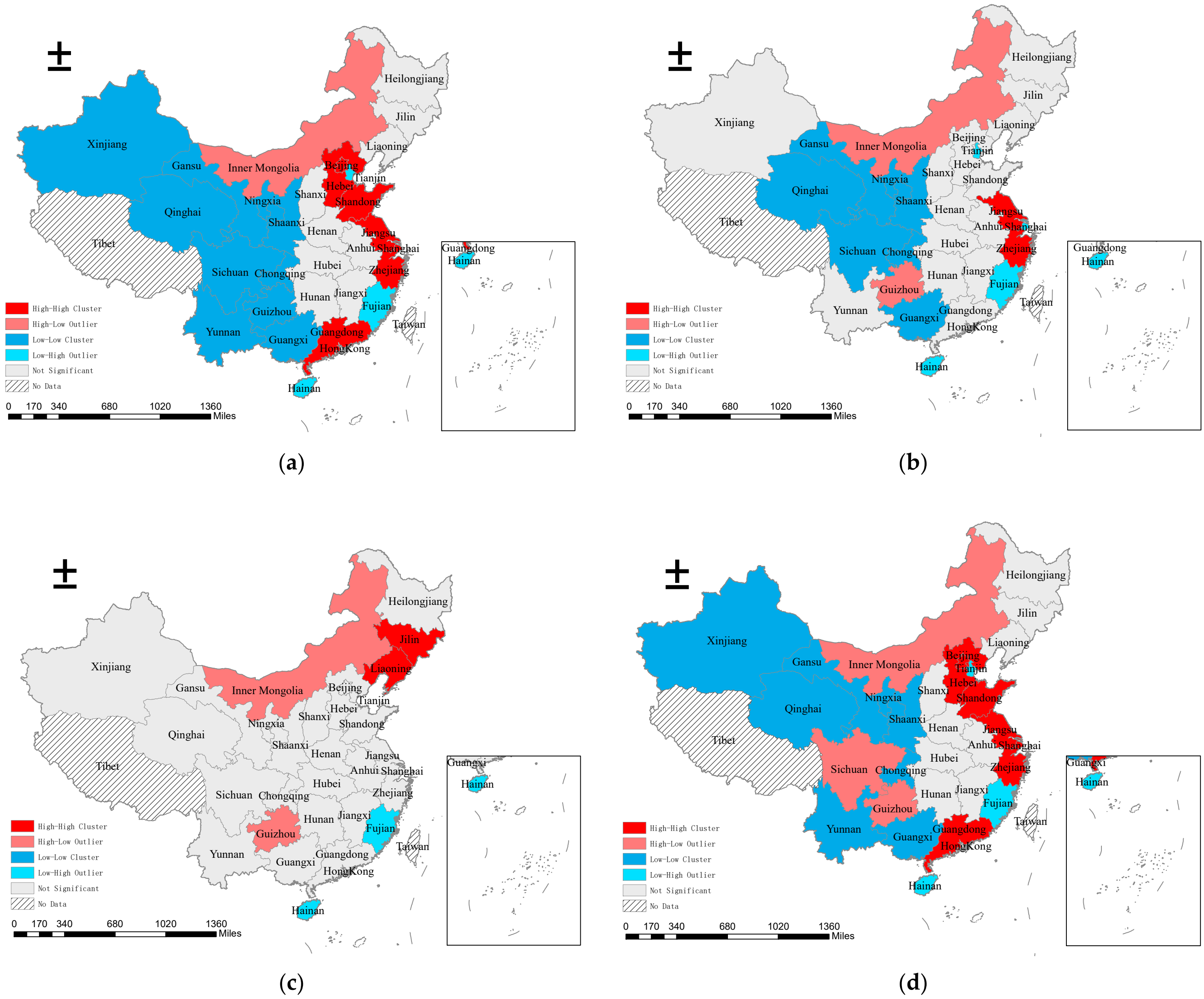

Figure 9. Aggregated distribution map of urban public buildings carbon emissions: (**a**) Cluster conditions in 2006; (**b**) Cluster conditions in 2010; (**c**) Cluster conditions in 2015; (**d**) Cluster conditions in 2019.

The spatial clustering characteristics of most provinces in the eastern coastal region and western provinces show a relatively stable trend. The coastal regions provinces like Shanghai, Jiangsu, and Zhejiang have consistently remained in the H-H cluster, while western regions provinces like Qinghai, Gansu, Shaanxi, Ningxia, and Chongqing have consistently been in the L-L cluster. Fujian, being close to the high-emission area, belongs to the L-H type. Inner Mongolia belongs to the H-L type, with significantly higher carbon emissions than surrounding provinces. Sichuan and Guizhou have shifted away from the L-L cluster to the H-L type, possibly due to accelerated urbanization, increased affluence of residents, increased energy consumption, and the formation of high-emission areas.

Overall, the spatial clustering types of urban public buildings carbon emissions are arranged from east to west, with a relatively stable spatial pattern. The H-H cluster is mainly gathered in the eastern region, whereas the L-L cluster is mainly gathered in the western region.

This distribution pattern can be attributed to the varying levels of development in China's eastern coastal and western inland regions. The eastern coastal provinces represent the more developed regions, while the inland provinces in the west are considered relatively underdeveloped. As a result, the coastal provinces in the east have consistently higher urban public buildings carbon emissions, while the inland provinces in the west maintain lower urban public buildings carbon emissions.

4.4. Driving Factors Decomposition Analysis

According to Kaya Identity, six contributors to carbon emissions from urban public buildings were selected: energy efficiency, energy consumption intensity, economic density, per capita urban public building area, urbanization, and population.

Table 3 provides decomposition results of every driving factor which was calculated based on the LMDI decomposition formula.

Overall, there was an enormous rise of 437.83 million tons in urban public buildings carbon emissions between 2006 and 2019, with a remarkable growth rate of 112.78%. Except for a slight slowdown in CO_2 emission growth in 2011 and 2014, carbon emissions increased to varying degrees in all other years and showed a growth-decline-stability trend.

Figure 10 provides an overview of the contribution level of driving factors to urban public buildings carbon emissions.

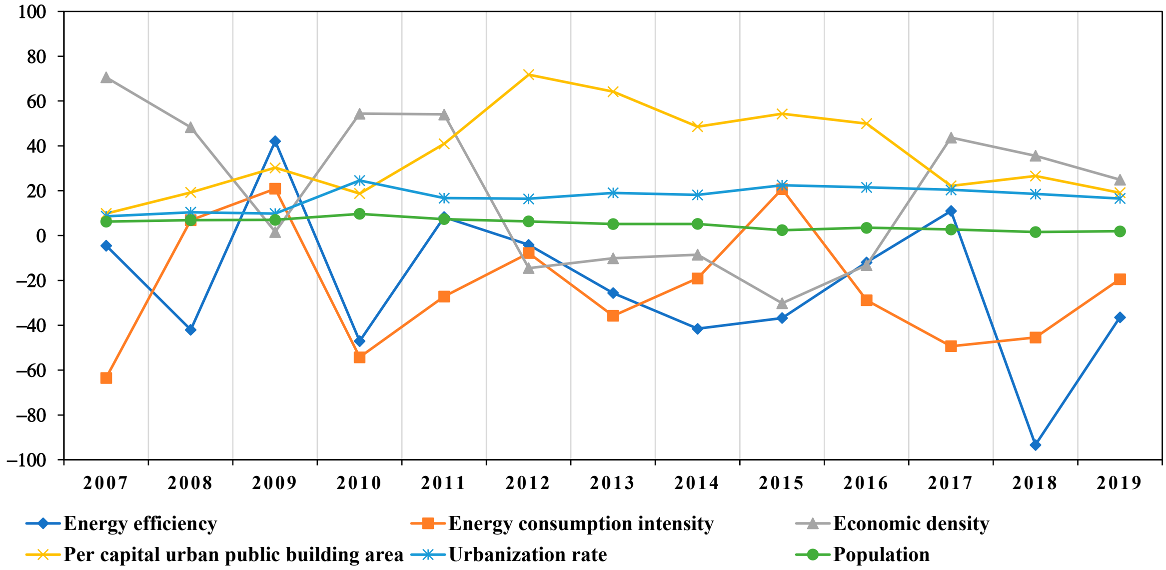

Figure 10. Contributions of driving factors to urban public buildings carbon emissions during 2006–2019.

(1) Energy consumption intensity and energy efficiency are negative driving factors affecting urban public buildings carbon emissions. Energy consumption intensity, which reflects the relationship between energy consumption and economic growth, plays a vital role in reducing carbon emissions. It stands out as the foremost factor contributing to the decline in urban public buildings carbon emissions. From 2006 to 2019, energy consumption intensity cumulatively reduced urban public buildings carbon emissions by 301.97 million tons, with a cumulative negative driving contribution rate of 51.71%. The rise for energy consumption intensity between 2007 and 2009 mitigates the growth in carbon emissions. Additionally, energy efficiency, as a negative driving factor, contributed to a cumulative contribution rate of 48.29% and stand out as another crucial contributor for decreasing urban public buildings carbon emissions.

Table 3. Decomposition results of driving factors of urban public buildings carbon emissions in 2006–2019 (million tons).

Driving Factors	2006–2007	2007–2008	2008–2009	2009–2010	2010–2011	2011–2012	2012–2013	2013–2014	2014–2015	2015–2016	2016–2017	2017–2018	2018–2019	Total
Energy efficiency	−4.50	−42.01	42.09	−47.06	8.28	−4.14	−25.63	−41.56	−36.74	−11.91	10.98	−93.37	−36.43	−282.00
Energy consumption intensity	−63.46	6.91	20.89	−54.25	−27.15	−7.80	−35.74	−19.05	20.75	−28.87	−49.32	−45.45	−19.44	−301.97
Economic density	70.58	48.32	1.64	54.38	54.00	−14.49	−10.12	−8.54	−30.19	−13.19	43.73	35.59	24.95	256.67
Per capita urban public building area	9.86	19.22	30.24	18.78	40.92	71.81	64.20	48.57	54.28	49.97	22.20	26.59	19.14	475.78
Urbanization rate	8.64	10.42	9.84	24.57	16.74	16.39	19.03	18.16	22.47	21.51	20.38	18.54	16.56	223.26
Population	6.25	6.90	7.04	9.68	7.37	6.32	5.16	5.20	2.45	3.49	2.73	1.59	1.91	66.09
Cumulative contribution value	27.38	49.77	111.74	6.10	100.17	68.09	16.90	2.77	33.03	21.00	50.71	−56.51	6.68	437.83

(2) Economic density, per capita urban public building area, urbanization rate, and population all have positive driving impact on the variation of urban public buildings carbon emissions. Among these positive driving factors, per capita urban public building area contributed to a cumulative increase of 475.78 million tons, with a positive driving contribution rate of 46.56%. Economic density and urbanization rate contributed to a cumulative increase of 256.67 million tons and 223.26 million tons. The combined positive driving contribution rate of the two factors accounted for 46.97%. The population had a relatively small contribution rate to urban public buildings carbon emissions, amounting to 6.47%. In terms of trends, the urbanization rate, population, and per capita public building area showed a stable tendency.

Figure 11 presents the spatiotemporal LMDI results of the comprehensive effect of six factors on urban public buildings carbon emissions across 30 provinces. Regarding the driving factors for urban public buildings carbon emissions in each province, per capita urban public building area, urbanization rate, population, and economic density exhibit positive impact.

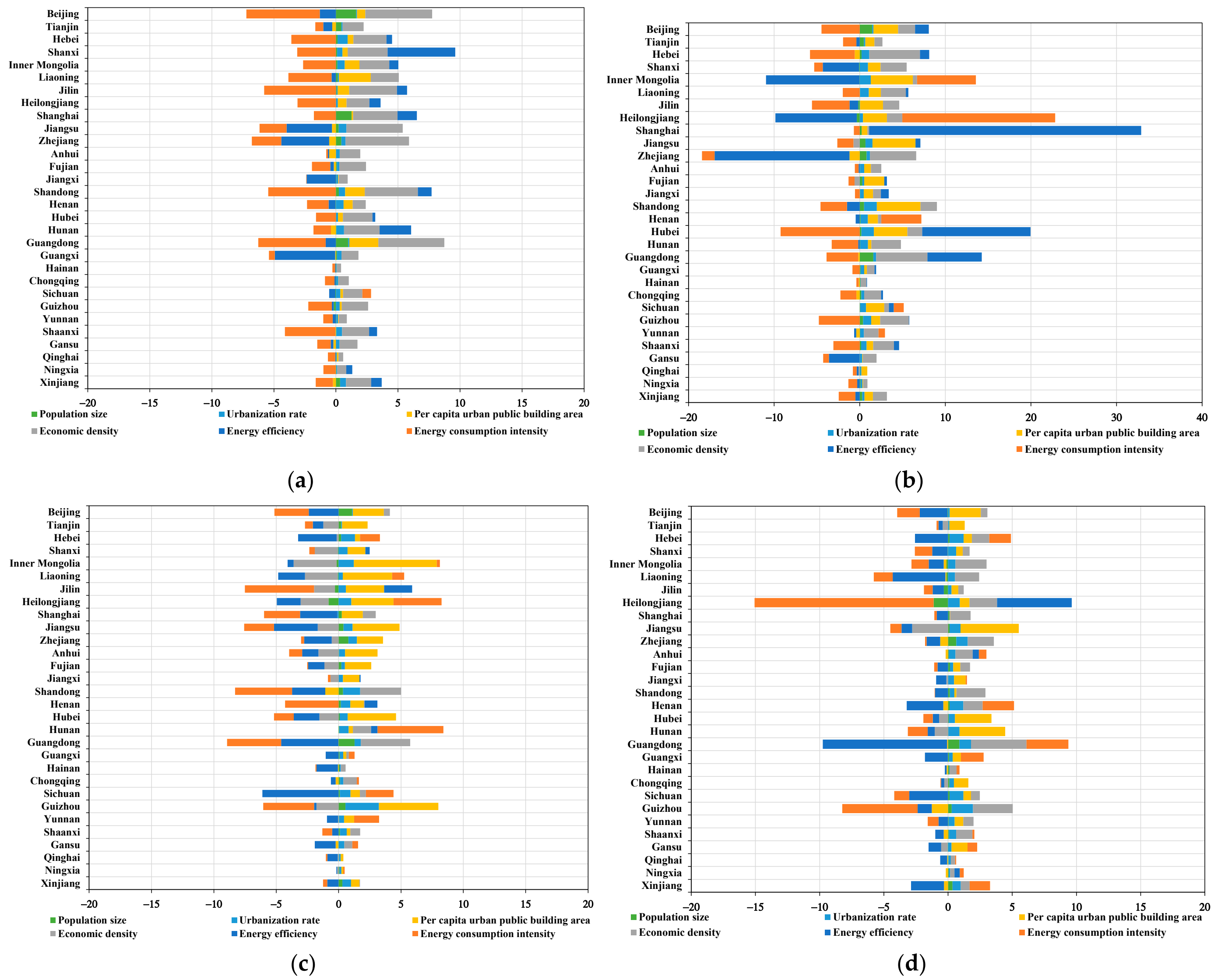

Figure 11. Temporal and spatial LMDI results of urban public buildings carbon emissions in 30 provinces: (**a**) 2007; (**b**) 2011; (**c**) 2015; (**d**) 2019.

Per capita urban public building area is recognized as a key factor contributing to the unequal urban public buildings carbon emissions in various provinces. The impact of per capita urban public building area on urban public buildings carbon emissions was relatively small from 2006 to 2007. However, as the building industry experienced quick growth in recent years, the impact of per capita urban public building area was significantly substantial in 2019. It has a positive impact on eastern coastal regions and has a constraining impact on western regions. It is worth noting that the acceleration of urbanization process, the advancement of urban construction and investment, and the continued expansion of building industry have led to an increase in per capita urban public building area, and ultimately resulting in higher carbon emissions.

The urbanization rate moderately contributes to the variations in urban public buildings carbon emissions among provinces. Provinces with a higher urbanization rate possess a larger and more positive effect. A higher urbanization rate signifies more energy-intensive urban public buildings, which promote energy-consuming activities including lighting, heating, air conditioning, and heating. As a result, urban public buildings carbon emissions increase rapidly.

The effect of population on the inequality of urban public buildings carbon emissions among various provinces is relatively small and shows a decreasing trend.

It can be observed from Figure 11 that provinces with larger populations, including Guangdong, Zhejiang, Shanghai, and Beijing, exhibit a significant population effect, resulting in increased urban public buildings carbon emissions. Similarly, provinces like Jiangsu, Hebei, Henan, and Sichuan, also with larger populations, experienced a rapid increase in carbon emissions.

Economic density is another factor that influence the inequality of urban public buildings carbon emissions. Economic density is a composite driving factor, which means that it has a facilitating effect in some areas and an inhibitory effect in others. In 2006, economic density had a promoting effect on urban public buildings carbon emissions for 30 provinces. In 2019, the number of provinces where economic density promoted carbon emissions was reduced to 22. Overall, there was a declining trend. With rapid socio-economic development, the swift expansion of urban public building areas and increased economic activities result in a higher economic density and carbon emissions, at the expense of enormous energy consumption.

Energy consumption intensity is a relatively large influence factor in suppressing urban public buildings carbon emissions. Provinces, where energy consumption intensity has a positive effect, are mainly located in western regions, including Inner Mongolia, Ningxia, Gansu, Yunnan, and Guangxi. These provinces are mainly resource-intensive areas, except for Guangxi Province, where the energy structure is mainly coal. In recent years, these areas have experienced rapid socio-economic development, resulting in high energy consumption intensity. In contrast, well-developed provinces like Beijing, Jiangsu, and Guangdong exhibit a substantial negative effect. It is widely recognized that these provinces have significantly optimized their energy structure, featuring a higher amount of clean energy sources.

Energy efficiency stands out as the primary factor responsible for suppressing urban public buildings carbon emissions, compared to other contributing factors. In 2006, energy efficiency had a suppressing impact in 18 provinces, while in 2019, it had a suppressing impact in 27 provinces. This indicates that energy efficiency has been gradually improving in several provinces, leading to a steady trend in urban public buildings carbon emissions. It is worth noting that this factor has a relatively small promoting effect in provinces such as Hubei and Shaanxi and a significant promoting effect in northern provinces such as Heilongjiang, Jilin, and Inner Mongolia. This may be attributed to their cold climate, where coal-fired centralized heating is used for an extended period. Additionally, these regions have a large consumption of coal and lower efficiency. Despite the extensive decline in the proportion of coal consumption, the rise in high-carbon electricity and heat generation remains unfavorable for carbon emissions reduction. Therefore, these northern regions need to focus on optimizing the energy structure of centralized heating and encouraging the adoption of new energy generation methods.

In conclusion, the results demonstrate that energy efficiency and energy consumption intensity play pivotal roles as driving factors in suppressing urban public buildings carbon emissions. Urbanization rate and population contribute stably to urban public buildings carbon emissions. Per capita urban public building area has become a main contributing driving factor in the increase in carbon emission levels, and its influence continues to strengthen.

Over the last two decades, China's socio-economic landscape is witnessing great development, accompanied by a fast urbanization process and frequent of economic activities. Economic density is a positively driving factor for urban public buildings carbon emissions and exhibits a decreasing trend.

The energy structure of urban public buildings between 2006 and 2019 is set out in Figure 12. It is evident that electricity, heating, and coal contribute to the vast majority of urban public buildings carbon emissions, accounting for approximately 90%. From another perspective, the demand for natural gas, liquefied petroleum gas, and oil during the operational phase of urban public buildings is relatively minimal. Urban public buildings have relatively low proportions of oil, natural gas, and liquefied petroleum gas usage, while the proportion of electricity has been on the rise. It has grown from over 50% in 2006 to 65% in 2019. The urban public buildings carbon emissions generated via electricity have increased from 209.97 million tons in 2006 to 562.39 million tons in 2019. Compared to electricity, the proportions of coal and heating have gradually decreased. Up to now, electricity is the absolute primary source of urban public buildings carbon emissions and determines the future trajectory of carbon emissions. Therefore, the foremost effective measure to curbing urban public buildings carbon emissions lies in controlling electricity consumption.

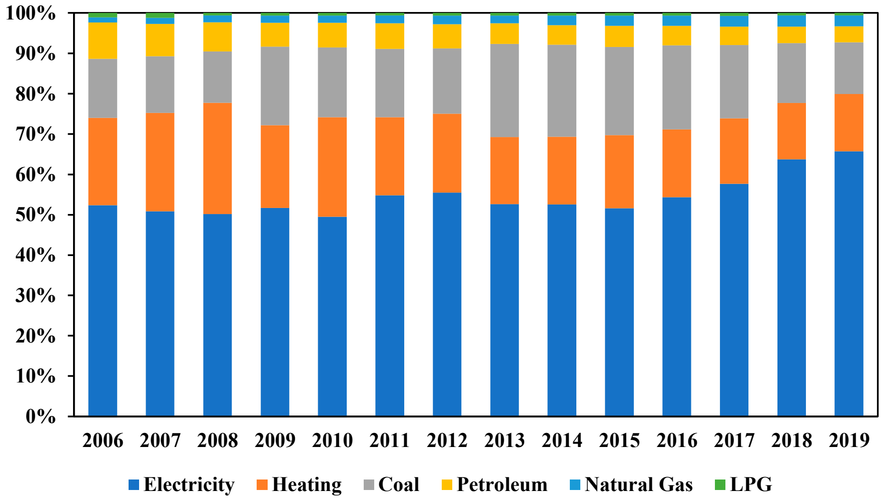

Figure 12. Energy structure of urban public buildings during 2006–2019.

5. Conclusions and Policy Suggestions

5.1. Main Findings

The building industry is crucial in addressing global warming due to its significant carbon emissions. This study investigates the spatiotemporal characteristics and regional differences of China's urban public buildings carbon emissions by using kernel density estimation, spatial autocorrelation analysis, and LMDI models. The influences of driving factors on the regional disparities were also quantified. This study offers a novel perspective on the driving factors affecting carbon emissions related to building energy, which holds significant importance for controlling carbon emissions from urban public buildings. Furthermore, it represents the first attempt in the field of urban public buildings carbon emissions. The findings are summarized below.

1. From 2006 to 2019, China's urban public buildings carbon emissions exhibited a consistent upward trend, reaching 401 million tons in 2006 and 853.23 million tons in 2019. The top-ranking regions in 2019 (Guangdong, Shandong, Heilongjiang, Jiangsu, and

Hebei) accounted for nearly 32% of the total emissions. However, the proportions of Ningxia (0.67%), Qinghai (0.8%), and Hainan (0.82%) were less than 2.5% of the total. The provinces experiencing quick growth were primarily concentrated in coastal and economically developed regions, whereas provinces with moderate growth were concentrated in central and northeastern regions. The provinces with slow development were mainly located in the underdeveloped regions of the southwest and northwest. The results show that there are great regional disparities in urban public buildings carbon emissions among provinces.

2. The regional disparities in urban public buildings carbon emissions have been gradually increasing. The kernel density estimation curve of 2006 showed a unimodal distribution with the center leaning towards the left. In 2010 and 2015, the summit of the kernel density curve exhibited a gradual decline, and the center shifted to the right. In 2019, the number of areas with high carbon emission values gradually increased. The shape of the kernel density curve exhibited a transformation from being tall and thin to short and wide, indicating an increasing regional disparity in urban public buildings carbon emissions. According to spatial autocorrelation analysis, the spatial positive correlation of urban public buildings carbon emissions is weakening. The spatial pattern of carbon emissions from urban public buildings is primarily characterized by significant high-high clusters provinces. Moreover, the spatial pattern remains relatively steady, and was characterized by significant high-high clusters in northeast and north China regions and low-low clusters in western regions.
3. Per capita urban public building area, economic density, urbanization rate, and population are the driving factors for urban public buildings carbon emissions. Their impacts on carbon emissions from urban public buildings decreased successively. Energy efficiency and energy consumption intensity are the major driving factors for reducing urban public buildings carbon emissions. Due to regional disparities in development, different regions showed different sensitivity to these factors. In the northeastern region, energy consumption intensity provides a considerable negative influence on urban public buildings carbon emissions. In the western and central regions, per capita urban public building area and urbanization rate shows a strong promoting influence on urban public buildings carbon emissions. In the eastern coastal region, both economic density and population contribute positively to urban public buildings carbon emissions. Furthermore, energy efficiency and energy consumption intensity exert the suppressing effect on urban public buildings carbon emissions.

5.2. Policy Suggestions

The above results are significant and meaningful for policymakers in implementing measures to decrease building carbon emissions and promote sustainable development. The policy suggestions are proposed as follows.

Improving Operational Energy Efficiency and Electrification of Urban Public Buildings: The government should actively enhance energy utilization efficiency and increase electrification in the operation phase of urban public buildings, while promoting the adoption of green electricity. Urban public buildings primarily rely on coal and electricity during operation, resulting in significant carbon emissions. However, it is widely recognized that electricity has a lower carbon emission factor compared to coal. Therefore, the government should actively promote the substitution of coal with electricity for end-use consumption in public buildings as an effective strategy to mitigate carbon emissions from urban public buildings.

Promoting Clean Energy and Energy-Efficient, Low-Carbon Building Technologies: The government should prioritize the transition to clean energy sources and consumption patterns, increasing the share of clean energy in electricity generation. Currently, the proportion of clean energy in electricity generation is relatively low. Efforts should be directed towards establishing a comprehensive clean energy supply system and investing in renewable energy sources such as solar and wind power. In addition, advocating for low-carbon and energy-efficient consumption patterns will create an environment conducive to the low-carbon operation of public buildings. Raising awareness of low-carbon consumption and guiding the public towards adopting a low-carbon lifestyle are essential for fostering sustainable development.

Develop Tailored Carbon Reduction Policies for Each Region: Urban public buildings carbon emissions among provinces are imbalanced, and the disparities across different regions can be attributed to distinct geographical locations, levels of economic development, and the openness of each region. It is recommended to develop specific policies and reduction targets based on the unique circumstances of each region. Specifically, efforts should be made to adapt region-specific methods for decreasing urban public buildings carbon emissions and foster collaboration among cities. In cold regions with high heating demands, enhancing heating efficiency through upgrading walls, roofs, and windows of public buildings is paramount. Additionally, the northeastern region should prioritize promoting waste heat recovery and exploring geothermal and solar energy as alternatives to coal-based heating. In central and western regions, it is advisable to focus on decreasing the reliance on coal consumption in public buildings' operation phase and increasing the adoption of electricity and wind energy. In the eastern coastal region, continual improvement should be placed on economic development and the continuous enhancement of high-tech industries and autonomous innovation capabilities.

The building industry has always been of great concern in energy conservation and emission reduction due to its importance and complexity. This study has some methodological and data limitations. The calculation results were conducted at the provincial level, without considering the differences among various cities. The data for urban public buildings carbon emissions are available up to 2019, as the data for 2020 and 2021 have not been published yet. However, the current findings can provide new insights for formulating appropriate urban emission reduction policies and low-carbon strategies. Future research should consider integrating multiple sources of data to compensate for the limitations of statistical data. The scope of the study should be narrowed down to focus on analyzing the urban public buildings carbon emissions in different cities. Furthermore, this research discovered that identical factors yield distinct effects in various regions. It is advisable for future research to focus on exploring the mechanisms by which different factors influence carbon emissions from urban public buildings.

Author Contributions: Conceptualization, Y.L. and Z.Z.; Methodology, Z.Z.; Software, T.M.; Data curation, T.M.; Visualization, T.M.; Writing—original draft preparation, Z.Z.; Writing—review and editing, Z.Z.; Supervision, Y.L.; Project administration, Y.L.; Funding acquisition, Y.L.; All authors have read and agreed to the published version of the manuscript.

Funding: This research was funded by National Natural Science Foundation of China, grant number 71871014.

Institutional Review Board Statement: Not applicable.

Informed Consent Statement: Not applicable.

Data Availability Statement: The data used to support the results are available from the corresponding author upon request.

Conflicts of Interest: All the authors declare no conflict of interest.

References

1. He, J.; Yue, Q.; Li, Y.; Zhao, F.; Wang, H. Driving force analysis of carbon emissions in China's building industry: 2000–2015. *Sustain. Cities Soc.* **2020**, *60*, 102268. [CrossRef]
2. Chen, C.; Bi, L. Study on spatio-temporal changes and driving factors of carbon emissions at the building operation stage—A case study of China. *Build. Environ.* **2022**, *219*, 109147. [CrossRef]
3. Zhu, C.; Chang, Y.; Li, X.; Shan, M. Factors influencing embodied carbon emissions of China's building sector: An analysis based on extended STIRPAT modeling. *Energy Build.* **2021**, *255*, 111607. [CrossRef]
4. BP. *BP Statistical Review of World Energy 2021*; BP: London, UK, 2021.

5. Mallapaty, S. How China could be carbon neutral by mid-century. *Nature* **2020**, *586*, 482–483. [CrossRef] [PubMed]
6. CABEE. *Annual Research Report on China's Building Energy Consumption 2021*; China Association Building Energy Efficiency: Beijing, China, 2021.
7. Zhang, S.; Ma, M.; Li, K.; Ma, Z.; Feng, W.; Cai, W. Historical carbon abatement in the commercial building operation: China versus the US. *Energy Econ.* **2022**, *105*, 105712. [CrossRef]
8. CABEE. *2022 Research Report of China Building Energy Consumption and Carbon Emissions*; China Association Building Energy Efficiency: Chongqing, China, 2022.
9. You, K.; Yu, Y.; Cai, W.; Liu, Z. The change in temporal trend and spatial distribution of CO_2 emissions of China's public and commercial buildings. *Build. Environ.* **2023**, *229*, 109956. [CrossRef]
10. Zhou, N.; Khanna, N.; Feng, W.; Ke, J.; Levine, M. Scenarios of energy efficiency and CO_2 emissions reduction potential in the buildings sector in China to year 2050. *Nat. Energy* **2018**, *3*, 978–984. [CrossRef]
11. Huo, T.; Xu, L.; Liu, B.; Cai, W.; Feng, W. China's commercial building carbon emissions toward 2060: An integrated dynamic emission assessment model. *Appl. Energy* **2022**, *325*, 119828. [CrossRef]
12. Lu, M.; Lai, J. Review on carbon emissions of commercial buildings. *Renew. Sustain. Energy Rev.* **2019**, *119*, 109545. [CrossRef]
13. Ma, M.; Yan, R.; Cai, W. An extended STIRPAT model-based methodology for evaluating the driving forces affecting carbon emissions in existing public building sector: Evidence from China in 2000–2015. *Nat. Hazards* **2017**, *89*, 741–756. [CrossRef]
14. Miao, L.; Gu, H.; Zhang, X.; Zhen, W.; Wang, M. Factors causing regional differences in China's residential CO_2 emissions—Evidence from provincial data. *J. Clean. Prod.* **2019**, *224*, 852–863. [CrossRef]
15. McNeil, M.A.; Feng, W.; Can, S.d.l.R.d.; Khanna, N.Z.; Ke, J.; Zhou, N. Energy efficiency outlook in China's urban buildings sector through 2030. *Energy Policy* **2016**, *97*, 532–539. [CrossRef]
16. Han, M.; Liu, W.; Xie, Y.; Jiang, W. Regional disparity and decoupling evolution of China's carbon emissions by province. *Resour. Sci.* **2021**, *43*, 710–721. [CrossRef]
17. Li, X.; Wang, J.; Zhang, M.; Ouyang, J.; Shi, W. Regional differences in carbon emission of China's industries and its decomposition effects. *J. Clean. Prod.* **2020**, *270*, 122528. [CrossRef]
18. Wang, X.; Fan, F.; Liu, C.; Han, Y.; Liu, Q.; Wang, A. Regional differences and driving factors analysis of carbon emissions from power sector in China. *Ecol. Indic.* **2022**, *142*, 109297. [CrossRef]
19. Liu, J.; Li, S.; Ji, Q. Regional differences and driving factors analysis of carbon emission intensity from transport sector in China. *Energy* **2021**, *224*, 120178. [CrossRef]
20. Cui, Y.; Khan, S.U.; Deng, Y.; Zhao, M. Regional difference decomposition and its spatiotemporal dynamic evolution of Chinese agricultural carbon emission: Considering carbon sink effect. *Environ. Sci. Pollut. Res.* **2021**, *28*, 38909–38928. [CrossRef]
21. Liu, J.; Wang, M.J. Study on Calculation and Regional Difference of Carbon Emission of Urban Civil Buildings in China. In Proceedings of the 3rd International Workshop on Advances in Energy Science and Environment Engineering, Suzhou, China, 29–31 March 2019.
22. Wang, Y.; Wu, X. Research on High-Quality Development Evaluation, Space–Time Characteristics and Driving Factors of China's Construction Industry under Carbon Emission Constraints. *Sustainability* **2022**, *14*, 10729. [CrossRef]
23. Huo, T.; Li, X.; Cai, W.; Zuo, J.; Jia, F.; Wei, H. Exploring the impact of urbanization on urban building carbon emissions in China: Evidence from a provincial panel data model. *Sustain. Cities Soc.* **2020**, *56*, 102068. [CrossRef]
24. Li, H.; Qiu, P.; Wu, T. The regional disparity of per-capita CO_2 emissions in China's building sector: An analysis of macroeconomic drivers and policy implications. *Energy Build.* **2021**, *244*, 111011. [CrossRef]
25. Zhang, Y.; Yu, Z.; Zhang, J. Analysis of carbon emission performance and regional differences in China's eight economic regions: Based on the super-efficiency SBM model and the Theil index. *PLoS ONE* **2021**, *16*, e0250994. [CrossRef] [PubMed]
26. Liu, X.; Yang, X.; Guo, R. Regional Differences in Fossil Energy-Related Carbon Emissions in China's Eight Economic Regions: Based on the Theil Index and PLS-VIP Method. *Sustainability* **2020**, *12*, 2576. [CrossRef]
27. Gan, L.; Liu, Y.; Shi, Q.; Cai, W.; Ren, H. Regional inequality in the carbon emission intensity of public buildings in China. *Build. Environ.* **2022**, *225*, 109657. [CrossRef]
28. Chen, H.; Du, Q.; Huo, T.; Liu, P.; Cai, W.; Liu, B. Spatiotemporal patterns and driving mechanism of carbon emissions in China's urban residential building sector. *Energy* **2023**, *263*, 126102. [CrossRef]
29. Wang, S.; Liu, H.; Pu, H.; Yang, H. Spatial disparity and hierarchical cluster analysis of final energy consumption in China. *Energy* **2020**, *197*, 117195. [CrossRef]
30. Liu, H.; Song, Y. Financial development and carbon emissions in China since the recent world financial crisis: Evidence from a spatial-temporal analysis and a spatial Durbin model. *Sci. Total Environ.* **2020**, *715*, 136771. [CrossRef]
31. Wang, C.; Guo, Y.; Shao, S.; Fan, M.; Chen, S. Regional carbon imbalance within China: An application of the Kaya-Zenga index. *J. Environ. Manag.* **2020**, *262*, 110378. [CrossRef]
32. Li, W.; Dong, F.; Ji, Z. Research on coordination level and influencing factors spatial heterogeneity of China's urban CO_2 emissions. *Sustain. Cities Soc.* **2021**, *75*, 103323. [CrossRef]
33. Wang, S.; Huang, Y.; Zhou, Y. Spatial spillover effect and driving forces of carbon emission intensity at the city level in China. *J. Geogr. Sci.* **2019**, *29*, 231–252. [CrossRef]
34. Li, W.; Sun, W.; Li, G.; Cui, P.; Wu, W.; Jin, B. Temporal and spatial heterogeneity of carbon intensity in China's construction industry. *Resour. Conserv. Recycl.* **2017**, *126*, 162–173. [CrossRef]

35. Bai, J.; Qu, J. Investigating the spatiotemporal variability and driving factors of China's building embodied carbon emissions. *Environ. Sci. Pollut. Res.* **2021**, *28*, 19186–19201. [CrossRef] [PubMed]
36. Li, T.; Gao, H.; Yu, J. Analysis of the spatial and temporal heterogeneity of factors influencing CO_2 emissions in China's construction industry based on the geographically and temporally weighted regression model: Evidence from 30 provinces in China. *Front. Environ. Sci.* **2022**, *10*, 1057387. [CrossRef]
37. Gong, Y.; Song, D. Life Cycle Building Carbon Emissions Assessment and Driving Factors Decomposition Analysis Based on LMDI—A Case Study of Wuhan City in China. *Sustainability* **2015**, *7*, 16670–16686. [CrossRef]
38. Jiang, B.; Huang, B.; Zhang, H. Study on Influencing Factors of Construction Industry Carbon Emissions in Jiangsu Province Based on LMDI Model. *Environ. Sci. Technol.* **2021**, *44*, 202–212. [CrossRef]
39. Shahbaz, M.; Loganathan, N.; Muzaffar, A.T.; Ahmed, K.; Ali Jabran, M. How urbanization affects CO_2 emissions in Malaysia? The application of STIRPAT model. *Renew. Sustain. Energy Rev.* **2016**, *57*, 83–93. [CrossRef]
40. Nasir, M.A.; Canh, N.P.; Lan Le, T.N. Environmental degradation & role of financialisation, economic development, industrialisation and trade liberalisation. *J. Environ. Manag.* **2021**, *277*, 111471. [CrossRef]
41. Wang, S.; Zhu, X.; Song, D.; Wen, Z.; Chen, B.; Feng, K. Drivers of CO_2 emissions from power generation in China based on modified structural decomposition analysis. *J. Clean. Prod.* **2019**, *220*, 1143–1155. [CrossRef]
42. Su, B.; Ang, B. Structural decomposition analysis applied to energy and emissions: Some methodological developments. *Energy Econ.* **2012**, *34*, 177–188. [CrossRef]
43. Rose, A.; Casler, S. Input–Output Structural Decomposition Analysis: A Critical Appraisal. *Econ. Syst. Res.* **1996**, *8*, 33–62. [CrossRef]
44. Hong, J.; Li, C.Z.; Shen, Q.; Xue, F.; Sun, B.; Zheng, W. An Overview of the driving forces behind energy demand in China's construction industry: Evidence from 1990 to 2012. *Renew. Sustain. Energy Rev.* **2017**, *73*, 85–94. [CrossRef]
45. Liu, Y.; Wang, J.; Wang, X.; Wu, H.; Guo, F.; Song, Y. A study of CO_2 emissions in China's domestic construction industry based on non-competitive input-output. *Sustain. Prod. Consum.* **2022**, *32*, 743–754. [CrossRef]
46. Shi, Q.; Chen, J.; Shen, L. Driving factors of the changes in the carbon emissions in the Chinese construction industry. *J. Clean. Prod.* **2017**, *166*, 615–627. [CrossRef]
47. Xu, W.; Xie, Y.; Xia, D.; Ji, L.; Huang, G. A multi-sectoral decomposition and decoupling analysis of carbon emissions in Guangdong province, China. *J. Environ. Manag.* **2021**, *298*, 113485. [CrossRef] [PubMed]
48. Wu, P.; Song, Y.; Zhu, J.; Chang, R. Analyzing the influence factors of the carbon emissions from China's building and construction industry from 2000 to 2015. *J. Clean. Prod.* **2019**, *221*, 552–566. [CrossRef]
49. Zheng, X.; Lu, Y.; Yuan, J.; Baninla, Y.; Zhang, S.; Stenseth, N.C.; Hessen, D.O.; Tian, H.; Obersteiner, M.; Chen, D. Drivers of change in China's energy-related CO_2 emissions. *Proc. Natl. Acad. Sci. USA* **2020**, *117*, 29–36. [CrossRef] [PubMed]
50. Ang, B.W. The LMDI approach to decomposition analysis: A practical guide. *Energy Policy* **2005**, *33*, 867–871. [CrossRef]
51. Zhang, W.; Li, K.; Zhou, D.; Zhang, W.; Gao, H. Decomposition of intensity of energy-related CO_2 emission in Chinese provinces using the LMDI method. *Energy Policy* **2016**, *92*, 369–381. [CrossRef]
52. Ang, B.W. Decomposition analysis for policymaking in energy: Which is the preferred method? *Energy Policy* **2004**, *32*, 1131–1139. [CrossRef]
53. Ang, B.W.; Choi, K.-H. Decomposition of Aggregate Energy and Gas Emission Intensities for Industry: A Refined Divisia Index Method. *Energy J.* **1997**, *18*, 59–73. [CrossRef]
54. Jiang, R.; Li, R. Decomposition and Decoupling Analysis of Life-Cycle Carbon Emission in China's Building Sector. *Sustainability* **2017**, *9*, 793. [CrossRef]
55. Ma, M.; Yan, R.; Du, Y.; Ma, X.; Cai, W.; Xu, P. A methodology to assess China's building energy savings at the national level: An IPAT–LMDI model approach. *J. Clean. Prod.* **2017**, *143*, 784–793. [CrossRef]
56. Lin, B.; Liu, H. CO_2 mitigation potential in China's building construction industry: A comparison of energy performance. *Build. Environ.* **2015**, *94*, 239–251. [CrossRef]
57. Wang, Y.; Song, J.; Yang, W.; Fang, K.; Duan, H. Seeking spatiotemporal patterns and driving mechanism of atmospheric pollutant emissions from road transportation in china. *Resour. Conserv. Recycl.* **2020**, *162*, 105032. [CrossRef]
58. Lu, X.; Kuang, B.; Li, J. Regional difference decomposition and policy implications of China's urban land use efficiency under the environmental restriction. *Habitat Int.* **2018**, *77*, 32–39. [CrossRef]
59. Zhao, J.; Ji, G.; Yue, Y.; Lai, Z.; Chen, Y.; Yang, D.; Yang, X.; Wang, Z. Spatio-temporal dynamics of urban residential CO_2 emissions and their driving forces in China using the integrated two nighttime light datasets. *Appl. Energy* **2019**, *235*, 612–624. [CrossRef]
60. Long, R.; Shao, T.; Chen, H. Spatial econometric analysis of China's province-level industrial carbon productivity and its influencing factors. *Appl. Energy* **2016**, *166*, 210–219. [CrossRef]
61. Shi, K.; Chen, Y.; Yu, B.; Xu, T.; Chen, Z.; Liu, R.; Li, L.; Wu, J. Modeling spatiotemporal CO_2 (carbon dioxide) emission dynamics in China from DMSP-OLS nighttime stable light data using panel data analysis. *Appl. Energy* **2016**, *168*, 523–533. [CrossRef]
62. Su, Y.; Chen, X.; Li, Y.; Liao, J.; Ye, Y.; Zhang, H.; Huang, N.; Kuang, Y. China's 19-year city-level carbon emissions of energy consumptions, driving forces and regionalized mitigation guidelines. *Renew. Sustain. Energy Rev.* **2014**, *35*, 231–243. [CrossRef]

63. Meng, Q.; Zheng, Y.; Liu, Q.; Li, B.; Wei, H. Analysis of Spatiotemporal Variation and Influencing Factors of Land-Use Carbon Emissions in Nine Provinces of the Yellow River Basin Based on the LMDI Model. *Land* **2023**, *12*, 437. [CrossRef]
64. Huo, T.; Ren, H.; Zhang, X.; Cai, W.; Feng, W.; Zhou, N.; Wang, X. China's energy consumption in the building sector: A Statistical Yearbook-Energy Balance Sheet based splitting method. *J. Clean. Prod.* **2018**, *185*, 665–679. [CrossRef]